https://dx.doi.org/10.1016/j.jclepro.2023.138648

Dual responsive microwave heating-healing system in asphalt concrete incorporating coal gangue and functional aggregate

Dong Lu [a,b,c], Xi Jiang [a], Zhen Leng [a,*], Shaowei Zhang [a], Daiyu Wang [b,c], Jing Zhong [b,c,*]

[a] *Department of Civil and Environmental Engineering, The Hong Kong Polytechnic University, Hong Kong SAR*

[b] *School of Civil Engineering, Harbin Institute of Technology, Harbin, 150090, PR China*

[c] *Key Lab of Structures Dynamic Behavior and Control of the Ministry of Education (Harbin Institute of Technology), Harbin, 150090, PR China*

[*] *Corresponding author. E-mail addresses: zhen.leng@polyu.edu.hk (Z. Leng), zhongjing@hit.edu.cn (J. Zhong).*

Abstract

The development of multifunctional asphalt concrete with a high heating-healing capability has emerged as a crucial focus in achieving pavement maintenance and sustainable infrastructure. However, striking a balance between achieving a high healing efficiency without compromising mechanical strengths and preventing aggregation of functional additives has presented a challenge. To address this, a novel concept of a dual responsive microwave heating-healing system in asphalt concrete is proposed, which incorporates coal gangue (CG) and functional aggregates. By incorporating functional aggregates, a robust and functional skeleton structure can be established within the asphalt concrete, facilitating the healing of microcracks at the interfaces between aggregates and asphalt. Simultaneously, the inclusion of CG in the asphalt mixture facilitates the healing of microcracks within the mastic. Remarkably, the incorporation of dual functional additives in the optimized asphalt concrete results in only a marginal decrease of 2% in maximum tensile strength and 1.5% in crack resistance compared to plain porous asphalt samples. Furthermore, the optimized asphalt samples exhibit healing index values exceeding 60% after undergoing five damage-healing cycles. To develop heating-healing asphalt concrete, it is recommended to utilize 100% CG in combination with functional aggregates. This comprehensive approach takes into account the valuable reuse of CG powder, as well as the associated environmental and economic benefits. This study introduces a promising strategy for achieving a highly efficient heating-healing capability in asphalt concrete, presenting significant potential for its practical applications in the field of sustainable pavement engineering.

Keywords*:* Asphalt concrete; Self-healing; Coal gangue; Solid waste; Sustainable pavement

Abbreviations

CG: Coal Gangue

PG: Performance Grading

CNT: Carbon Nanotube

CNTP: CNT-Polymer

LM: Limestone Mineral

PA: Porous Asphalt

SEM: Scanning Electron Microscopy

SCB: Semi-Circular Bending

HI: Healing Index

3D: Three-Dimensional

SD: Standard Deviations

UTM: Universal Testing Machine

1. Introduction

Asphalt pavements commonly exhibit various forms of deterioration or distress over their extended lifespan, resulting from factors such as traffic loads and environmental conditions (Alvarez et al., 2011; Taheri-Shakib and Al-Mayah, 2023; Tian et al., 2020). Among these, cracks are the leading cause of pavement deterioration (Jiang, J. et al., 2022; Karimi et al., 2021; Xiao et al., 2022). Generally, cracks in asphalt concrete can be classified into two types: cohesive failure, which originates from the chemical bond breaking between asphalt molecules (Li, B. et al., 2023; Meng et al., 2023; Song et al., 2023; Zhang et al., 2023), and adhesive failure, typically caused by the separation of asphalt-aggregate bonds (Cong et al., 2023; Huang et al., 2023). Cracking significantly impacts the service life of asphalt pavements (Jiang, X. et al., 2022b; Jiang, X. et al., 2022c), thus leading to increased maintenance costs (Franesqui et al., 2017; García, 2012; Jiang, X. et al., 2022a). Consequently, the detection and repair of cracks in asphalt concrete have garnered significant attention in recent years, contributing to preserving and potentially restoring the performance and serviceability of asphalt pavements (Amani et al., 2020; Amin and Esmail, 2017; Song et al., 2022b).

Asphalt binder is a self-healing material (Dai et al., 2013; Gallego et al., 2021), which can repair micro-cracks in asphalt concrete during rest periods between loading cycles (Fu et al., 2022; García et al., 2013). However, this inherent self-healing ability is limited due to frequent traffic flow. It is widely acknowledged that the crack-healing efficiency of asphalt concrete can be enhanced by raising the temperature of cracked concrete with the aid of microwave radiation (Jahanbakhsh et al., 2018; Karimi et al., 2018). Several studies have suggested that incorporating metal-based or carbon-based additives into the asphalt binder and combining them with raw aggregates (fillers) can improve the heating-healing capability of asphalt concrete (Li et al., 2018; Wang et al., 2022; Wang et al., 2016; Yoo et al., 2019). Nonetheless, dispersing these additives into the asphalt poses challenges (Lu, D. et al., 2023; Lu, Dong et al., 2023d; Lu et al., 2022a), as it is a time-consuming, labor-intensive, and expensive process, limiting the practical application (Lu, Dong et al., 2023c; Wang et al., 2022; Wang et al., 2016). Moreover, replacing mineral filler with heterogenous microwave-sensitive waste metal filler has been reported to enhance the heating-healing capability of asphalt concrete (Li et al., 2022; Yıldız and Atakan, 2020; Zhu et al., 2019). However, since asphalt and filler constitute only a small volume of asphalt concrete (~5%), enabling heating-healing efficiency is limited. Furthermore, both approaches face difficulties in achieving proper dispersion of the added functional additives (Lu et al., 2022c), and they primarily address cohesive failure.

Among the typically used waste fillers, coal gangue (CG) has low carbon levels derived from the process of coal mining (Hong et al., 2020; Moghadam et al., 2019). In China, CG accumulates in massive quantities, with approximately 4.5 billion tons currently present and an annual output of 300-400 million tons (Moghadam et al., 2019). The long-term storage of CG not only occupies valuable land resources and affects the visual appeal of the environment but also poses significant pollution risks and health hazards to residents (Liu et al., 2023). CG has a similar particle size to the mineral filler and reusing it for developing asphalt concrete can save resources and avoid environmental hazards (Li, F. et al., 2023). Recent studies have explored the recycling CG as an alternative to conventional mineral fillers in asphalt (or asphalt concrete) to improve its rheological behavior (Li, F. et al., 2023), microstructure (Liu et al., 2023), and low-temperature crack resistance (Hong et al., 2020). More importantly, CG contains abundant microwave-sensitive inorganic and metal compositions, such as SiO_2, Fe_2O_3, CaO_2, MaO, K_2O, and Al_2O_3, enabling it to have the potential to absorb microwaves for heating and improve the heating-healing capability of asphalt concrete (Li et al., 2022). However, the exploration of CG powder in asphalt microwave self-healing is extremely limited.

Steel slag is the solid waste from the steelmaking process, which causes serious environmental pollution and safety hazards (Jiang, X. et al., 2023; Liu, Jianan et al., 2022). Thankfully, its high iron content enables it to have outstanding microwave heating capability for enhancing the microwave heating-healing properties of asphalt concrete (Phan et al., 2018). Recently, studies have demonstrated that steel slag can be used as a partial replacement for natural aggregate to primarily address adhesive failure caused by asphalt-aggregate debonding (Liu, Jinzhou et al., 2022; Liu, Jianan et al., 2022; Phan et al., 2018). The random distribution and dispersion of steel slags in asphalt concrete make them potentially suitable for achieving excellent uniformity under microwave radiation (Jiao et al., 2020). However, the sourcing (or quality) of steel slags is complex (or unstable), and there are limitations in transportation distance (Bai and Wang, 2023). Additionally, the high porosity of steel slags consumes more asphalt, and their density is 20-30% higher than that of natural aggregates, resulting in higher freight costs and increased investment (Jiang, Q. et al., 2023). These challenges have inspired the exploration of a novel functional aggregate capable of creating asphalt concrete with a three-dimensional functional skeleton structure.

Based on the above analysis, there is indeed a lack of comprehensive studies exploring the use of both functional aggregates and CG in the development of asphalt concrete with excellent microwave heating-healing capability. This research gap highlights the need for an urgent investigation into a novel

asphalt concrete that incorporates the concept of a dual-responsive microwave heating-healing system. To address this research gap, this study introduces the concept of a dual-responsive microwave heating-healing system in asphalt concrete, incorporating functional aggregates and CG. In this system, the inclusion of functional aggregates allows for the creation of a functional skeleton within the asphalt concrete, enabling the healing of microcracks at the interfaces between aggregates and asphalt. Simultaneously, the incorporation of CG in the asphalt mixture contributes to the healing of microcracks within the mastic. As a result, the optimized asphalt concrete incorporating these dual functional additives exhibits only a marginal decrease of 2% in maximum tensile strength and 1.5% in crack resistance compared to plain samples. Furthermore, the healing index values of these optimized asphalt samples exceed 60% after undergoing five damage-healing cycles. These findings offer a promising strategy for achieving highly efficient heating-healing capabilities in asphalt concrete and have significant potential for practical applications in the field of sustainable pavement engineering.

2. Materials and methods

2.1. Materials

Porous asphalt concrete (PA-13) with a nominal maximum aggregate size of 13.2 mm was selected as the base concrete for the modification of thermal conductivity, aiming to address the issue of ravelling in asphalt pavement (Jiang, J. et al., 2022). The aggregate gradation of crushed granite aggregates used in this study is depicted in **Fig. S1** (**Supporting Information**). To achieve the desired modification, a mixture of carbon nanotube (CNT) dispersion and polyacrylic acid solution was prepared using a high-speed mechanical shear machine. The prepared CNT-polymer nanocomposite (CNTP) was utilized to coat the surface of the aggregates, thereby producing functional aggregates. The detailed process for the preparation of functional aggregates will be elaborated upon in the subsequent section. An asphalt binder with a performance grading (PG) of 76 ºC was used and its basic properties are presented in **Table S1 (Supporting Information)**. Additionally, two types of fillers, namely limestone mineral (LM) powder and coal gangue (CG) powder, were used to prepare PA-13. The CG powder exhibits a dark-grey color due to its predominant coal content. The density of LM and CG is measured at 2.716 g/cm^3 and 2.643 g/cm^3, respectively. Furthermore, the specific surface area of LM and CG is found to be 0.23 m^2/g and 0.27 m^2/g, respectively.

2.2. Preparation of functional aggregates and mixture design

The deposition of a CNT functional film onto the aggregate surface was carried out prior to mixing with the asphalt binder and filler. The process involved synthesizing a well-dispersed CNTP mixture, as depicted in **Fig. S2**. To achieve this, the CNT dispersion with a solid content of 5% and the polyacrylic acid solution with a solid content of 48% were thoroughly mixed using a high-speed shear mixer. Specifically, the two components were stirred for 10 minutes at 2000 revolutions/minute (r/min), followed by an additional 20 minutes at 3000 r/min, based on our pre-experimental experience (Lu, Dong et al., 2023a). Subsequently, the raw aggregates were immersed in the well-dispersed CNTP mixture and manually stirred at a speed of 30-50 r/min for 10 minutes to ensure a uniform coating of CNTP on the aggregate surface. The volume of the CNTP mixture used should exceed that of the aggregates to ensure complete coverage of all the aggregates. The mixture was then dried in an oven at 80 ℃ for 24 hours to evaporate any remaining moisture, resulting in the deposition of the CNTP film on the aggregate surface. It is important to note that the concentration of CNT in the CNTP film was approximately 20 wt%, leading to severe agglomeration of CNT (Lu et al., 2022b). We believe that this characteristic is advantageous for the electrical conductivity of the CNTP film, as electrons can directly transport through the entangled CNT without the need for tunneling through the polymer medium in between (Lu et al., 2022f). However, if these CNTP mixtures were mixed with the asphalt binder, the inevitable agglomeration of nanomaterials could have negative effects (Lu et al., 2022d; Lu, Dong et al., 2023e), such as reducing mechanical properties and causing non-uniform microwave heating performance, as discussed in the subsequent sections.

PA concrete is known for its multifunctionality and environmental friendliness and has been widely used as a road surfacing material, particularly in high-density cities like Hong Kong (Jiang, J. et al., 2022). In this study, all the asphalt concrete samples were prepared following the *Chinese Technical Specifications for Construction of Highway Asphalt Pavements JTG/T 3350-03-2020*. The optimum asphalt content for the selected PA-13 mixture was determined using the Marshall method. It was found to be 3.9 wt%, and the target air void was set at (23±0.5)%. To compare the influence of functional aggregates on the self-healing properties of asphalt concrete, the same aggregate gradation and a constant asphalt content were used. In the case of self-healing asphalt concrete, the LM powder was replaced by CG powder in an equivalent volume. The mixture design of the asphalt concrete samples is presented in **Table 1**. The preparation process involved adding aggregates (or functional aggregates, if applicable), asphalt, and LM powder (or CG powder, if applicable) in a specific order into the mixing pot. These components were then stirred for 90 seconds to ensure thorough mixing. The mixture was then used to

prepare Marshall samples using a Marshall compactor. After compaction, the standard Marshall samples were left at room temperature for 24 hours. Finally, the samples were cut into semicircular slices with a diameter of approximately 150 mm and a thickness of approximately 50 mm. Each semicircular slice featured a middle notch with dimensions of 10 mm in width and 10 mm in height, which was created using a high-precision cutting saw.

Table 1 Asphalt concrete mix design (%).

Mixture ID	Binder	Aggregate		Filler	
		Raw	Functional	Limestone	Coal gangue
PA	3.9	100	-	100	0
PA-50CG	3.9	100	-	50	50
PA-100CG	3.9	100	-	0	100
PA-FAg	3.9	-	100	100	0
PA-FAg-50CG	3.9	-	100	50	50
PA-FAg-100CG	3.9	-	100	0	100

2.3. Test methods

2.3.1. Properties of raw materials

Scanning electron microscopy (SEM), utilizing the Tescan Mira4 instrument, was employed to observe the morphology of both aggregates and fillers. Prior to analysis, the aggregates (or fillers) underwent an oven-drying process at 60 ℃ for 48 hours. Subsequently, they were affixed onto a sample holder using a conductive adhesive and coated with a thin layer of gold via sputter-coating. Raman spectra were acquired using a confocal Raman spectrometer, specifically the Thermo Fischer DXR model, which employed a 532 nm laser excitation source. To determine the chemical compositions of the two types of fillers, an X-ray fluorescence spectrometer with a power of 4 kW and a maximum current of 160 mA was utilized.

2.3.2. Cracking resistance of asphalt concrete

A cracking resistance assessment of asphalt concrete samples was performed through a three-point bending test (**Fig. 1**). To achieve this, three circular discs were obtained by cutting from an original

specimen. Each disc was then divided into two semi-circular samples, resulting in a total of six semi-circular samples. The diameter and height of each semi-circular sample were 150 mm and 75 mm, respectively. The semi-circular bending (SCB) test was conducted using a Universal Testing Machine (UTM-100) machine. The test employed a constant loading rate of 0.5 mm/min and was carried out at a consistent temperature of 25 ℃. Prior to testing, all samples were placed in a temperature chamber at 25 ℃ for a minimum of 12 hours to ensure a stable temperature environment. The maximum tensile strength of the asphalt concrete serves as an indicator of its crack resistance (Amani et al., 2023; Beserra Costa et al., 2023; Erarslan, 2023; Song et al., 2022a; Song et al., 2021), can be calculated using **Eq. (1)**.

$$\sigma_t = \frac{4.236 \times P}{D \times T} \quad (1)$$

where σ_t is the maximum tensile strength (MPa), P is the maximum load (N), D is the sample diameter (mm), and T is the sample thickness (mm).

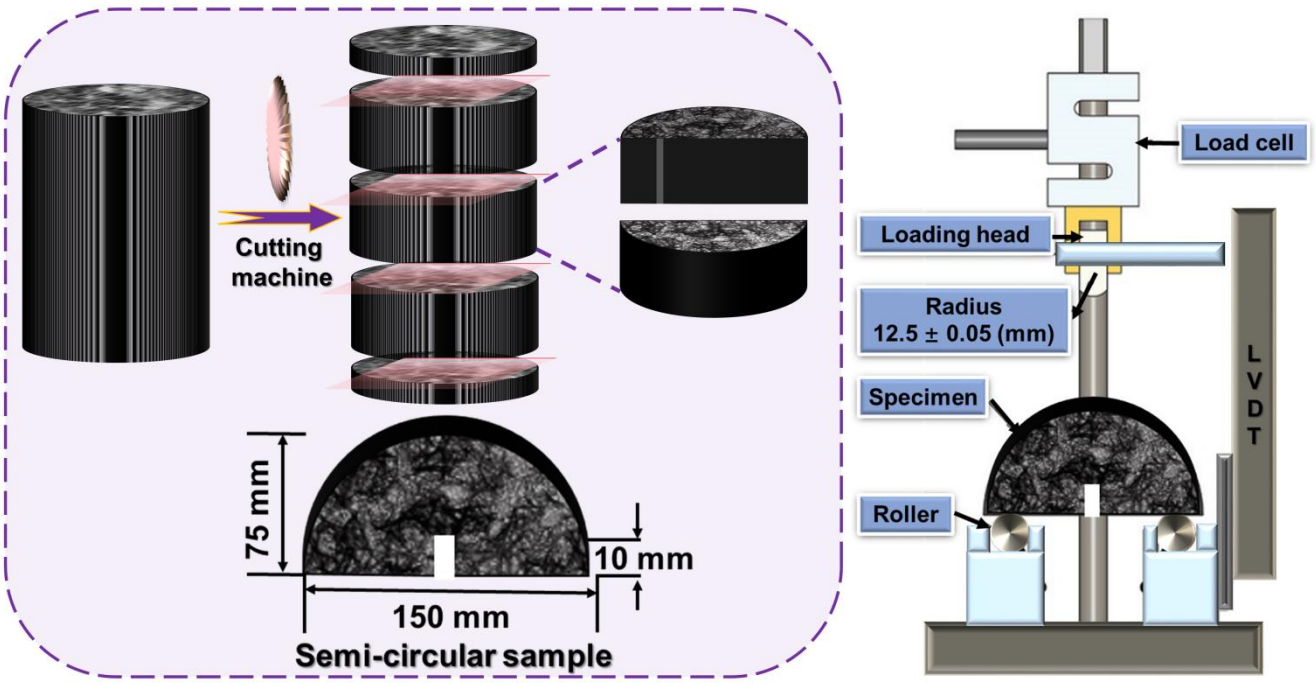

Fig. 1. Preparation of SCB samples and illustration of three-point bending test.

2.3.3. Evaluation of microwave heating characteristics of filler and asphalt concrete

The fillers and aggregates were heated in a microwave oven at 800 W for different durations (i.e., 0 s, 30 s, 60 s, 90 s, 120 s, 150 s, and 180 s) to measure their surface temperature using a handheld thermometer. Additionally, asphalt concrete samples were also heated in a microwave oven and a hand-held FLIR T650sc infrared thermal imager was used to measure the surface temperature. Specifically, the

samples were heated using different durations and constant power (800 W) to screen the optimal heating scheme for the following heating-healing process. Before conducting the tests, all samples were maintained at an ambient temperature to ensure an initial temperature. The microwave heating rate of the samples can be calculated by **Eq. (2)**.

$$V_{\mathrm{H}} = \frac{T - T_0}{t} \tag{2}$$

where V_{H} is the heating rate of asphalt concrete (℃/s), T and T_0 are the temperatures after heating and the initial temperature (℃), respectively, and t is the heating time (s).

2.3.4. Damage-healing-damage process

Fig. 2 illustrates the process of an SCB test conducted to generate a damaged sample containing a crack along the notch in the middle. Following the creation of the crack, the two pieces of the sample were reassembled and subjected to microwave radiation at 800 W. Subsequently, the samples were allowed to rest for 6 hours at room temperature. Finally, the samples underwent another round of testing through the SCB test, completing a damage-healing-damage cycle. The healing index (HI) can be obtained using **Eq. (3)**.

$$HI = \frac{F_1}{F_0} \times 100\% \tag{3}$$

where HI is the healing index (%); F_0 and F_1 are the maximum force initially tested and the maximum force measured after the healing (N), respectively.

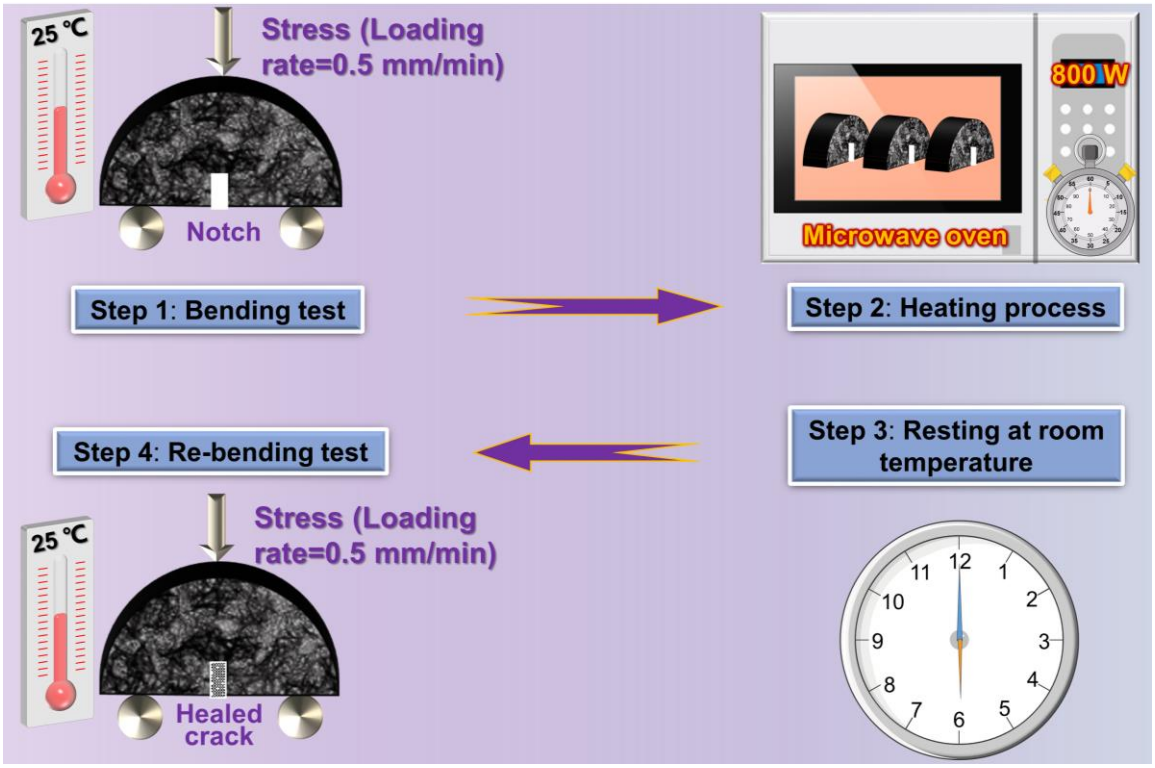

Fig. 2. Illustration of damage-healing-damage cycles of asphalt concrete samples.

3. Results and discussion

3.1. Properties of functional aggregates and fillers

3.1.1. Properties of functional aggregates

In this study, a polyacrylic acid solution was used as a polymer binder and combined with a CNT suspension to create a functional coating layer with exceptional microwave sensitivity and strong binding strength. Increasing the concentration of CNT in the CNTP enhances both the microwave sensitivity and modulus of the coating layer. Based on previous research (Lu, Dong et al., 2023a), a CNT concentration of approximately 20 wt% was selected for this study.

Fig. 3a displays the transformation of the raw aggregates during the dip-coating process. The top row shows the aggregates in their original grey color, while the bottom row demonstrates the highly uniform dark appearance after the dip-coating process. Moreover, SEM observation reveals that the morphology of the aggregates changes from a smooth surface with some debris to a rough layer of functional CNTP. The well-connected bundles of CNT can be identified, indicating the formation of a tightly coated functional CNTP film on the surface of the aggregates. The presence of protruding CNT in the coating layer is presumed to enhance interlocking between the asphalt-functional aggregates and promote direct

contact among the functional aggregates, thereby facilitating the construction of a well-connected three-dimensional (3D) functional skeleton. Furthermore, the Raman spectrum analysis (**Fig. 3b**) confirms the detection of CNT signals on the aggregate surface, particularly observing a prominent G/D peak and a relatively weak 2D peak. This further supports the formation of a functional CNT layer on the aggregate surface. **Fig. 3c** presents the results of the 24-hour water absorption test for the functional aggregates. It shows a slight decrease of approximately 5% in water absorption, primarily attributed to the hydrophobic nature of the CNT bundles (Lu et al., 2022e; Wang, Y. et al., 2020). Importantly, during the dry mixing and scratching process, almost no film was peeled from the aggregate surface (**Fig. S3, Supporting Information**), indicating excellent bonding quality between the functional CNTP layer and the aggregates.

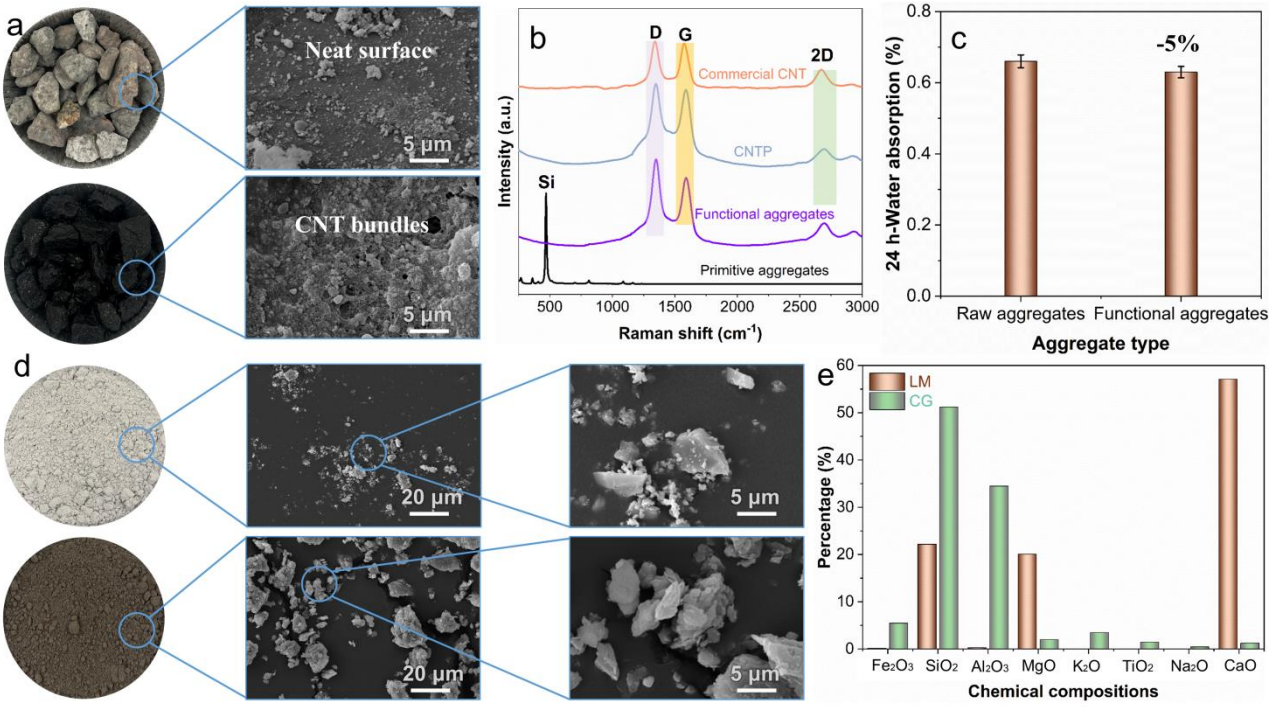

Fig. 3. Properties of raw materials: (a) the appearance and SEM observation of aggregates; (b) the Raman spectrum; (c) water absorption of aggregates; (d) the appearance and SEM observation of fillers; and their (e) chemical compositions.

3.1.2. Composition and morphology of functional filler

In **Fig. 3c**, the LM powder is depicted in grey-white color in the top row, while the CG powder exhibits a brown appearance due to its high coal content in the bottom row (Hong et al., 2020; Jiang et al., 2021; Li, F. et al., 2023; Moghadam et al., 2019; Wang et al., 2023). SEM observation reveals that the LM

powder displays a relatively smooth surface with irregular polyhedral shapes and fewer bumpy structures. It also exhibits open pores. On the other hand, CG powder exhibits a rough surface with a fluffy and irregular shape, along with pore holes and interstitial pores. The presence of carbon volatilization in CG powder leads to a more abundant pore structure (Li, F. et al., 2023; Li et al., 2022; Liu et al., 2023). Moreover, the bumpy or depressed structure of CG powder increases the contact area between the filler and asphalt binder, thereby enhancing interfacial bonding compared to LM powder (Hong et al., 2020; Li, F. et al., 2023). As presented in **Fig. 3d**, it is evident that the CG powder contains a higher concentration of active mineral components and metal oxides compared to the LM powder. These active minerals contribute to improving the bond between the asphalt and the filler, while metal oxides such as Fe_2O_3 and Al_2O_3 enable efficient microwave heating capabilities, ensuring fast heating (Guan et al., 2019).

3.2. Cracking resistance

The SCB test has been widely used to assess the cracking resistance of asphalt concrete, as recommended by previous literature (Mojabi et al., 2020; Salehi Ashani et al., 2022). This test offers several advantages, including low cost, easy sample preparation, and a simple test setup (Fakhri et al., 2023; Marín-Uribe and Restrepo-Tamayo, 2022). Its results are highly correlated with the performance of flexible pavement in the field (Lu, Dong et al., 2023b; Wang, J. et al., 2020). According to the continuum damage theory, the evaluation of damage in asphalt concrete is influenced by total strain, encompassing both viscoelastic and viscoplastic components (Cao et al., 2020). At low temperatures, asphalt concrete exhibits a high modulus of elasticity, resulting in predominantly elastic deformation and fracture-based damage. This leads to the formation of cracks with a rough surface (**Fig. 4a**, top) (Keshavarzi and Kim, 2016). On the other hand, at intermediate temperatures, asphalt concrete experiences significant viscoelastic and viscoplastic strains (Mulugeta Alamnie et al., 2022). This results in the induction of more microcracks due to viscoplastic strain and aggregate reorientations (**Fig. 4a**, bottom). Therefore, the SCB test at an intermediate temperature of 25 °C was chosen to evaluate the cracking resistance of asphalt concrete.

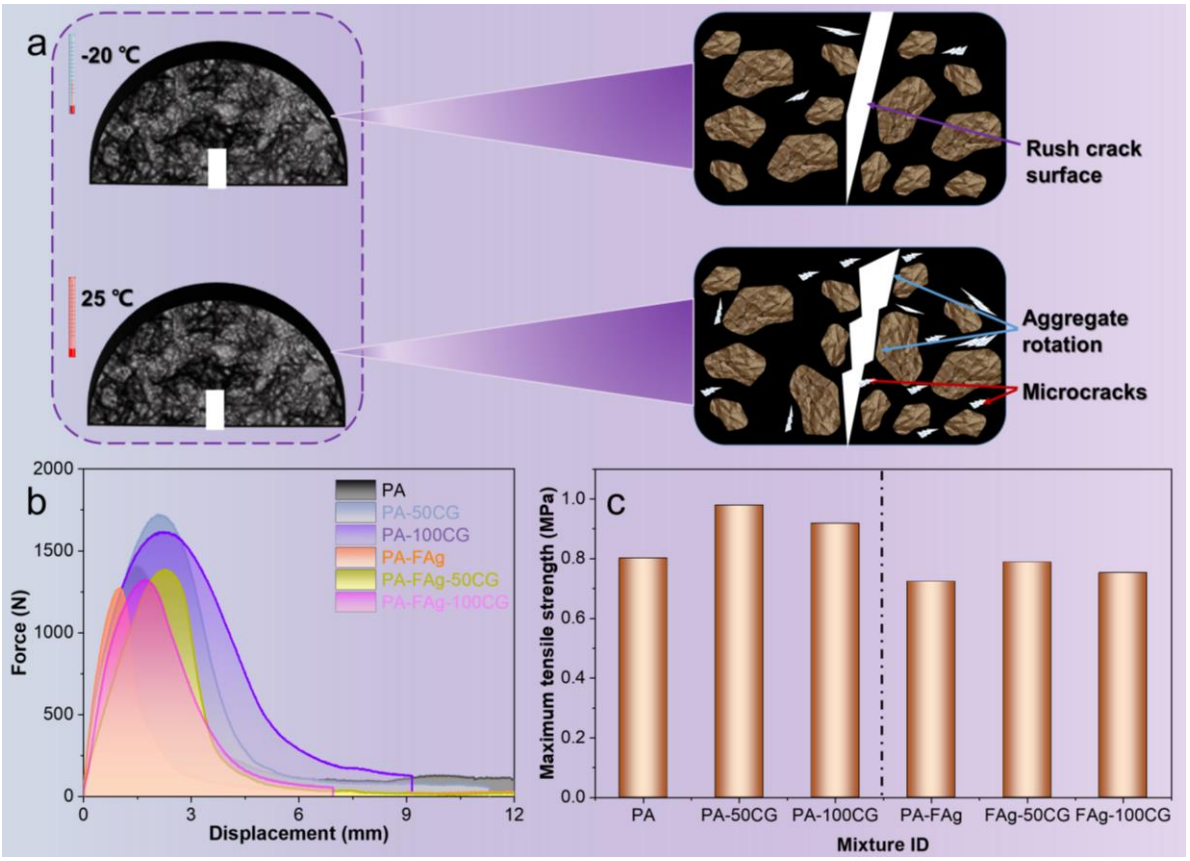

Fig. 4. (a) Illustration of crack propagation of asphalt concrete at different temperatures: crack at low temperature (top) and intermediate temperature (bottom); (b) load-displacement curves; and (c) maximum tensile strength.

As illustrated in **Fig. 4b**, the asphalt concrete containing 50% CG powder exhibited the highest applied force. The maximum force of the asphalt concrete modified with 100% CG powder was lower than that of the PA-50CG samples but still higher than the PA samples. In the case of the PA-50CG sample, the LM powder and CG powder were first mixed before being added to the asphalt concrete. This optimized the particle gradation of the fillers and refined the microstructure (Gan et al., 2021; Lu et al., 2021). Furthermore, the activated CG powder possesses a porous and loose structure, with protrusions and wrinkles that allow it to absorb more asphalt. The rough surface of the CG powder generates Van der Waals forces with the asphalt, which results in polarized molecular contact and induces an electric dipole moment. This forms a physical orientation layer, locks the asphalt orientation, and enhances the internal cohesion of the asphalt concrete (Hong et al., 2020). Based on these findings, the optimal replacement rate of CG powder in asphalt concrete is determined to be 50% for achieving the best crack resistance. The maximum force of the PA-FAg samples decreased by 9.8% compared to the plain PA samples. The calculation of the maximum tensile strength (0.72 MPa for PA-FAg samples and 0.80 MPa for plain PA samples, as shown in **Fig. 4c**) further confirms that the addition of functional aggregates slightly reduces

the crack resistance of the asphalt concrete. However, it is interesting to note that the combined usage of functional aggregates and CG powder can compensate for the strength loss observed when adding functional aggregates directly. These results indicate that the combined application of functional aggregates and functional CG powder in asphalt concrete provides acceptable strength and crack resistance for practical applications.

3.3. Microwave heating properties under radiation

3.3.1. Microwave heating capacity of functional additives

In **Fig. 5a**, the microwave heating capacity of two types of filler is compared. As anticipated, the temperature of the fillers increases with longer microwave irradiation time. Notably, the functional CG powder exhibits significantly higher temperatures compared to the LM powder at all heating durations. For the LM powder, the average temperature reaches only 27.7 ℃ and 63.8 ℃ after 30 s and 180 s of microwave radiation, respectively. In contrast, the average temperature of the CG powder reaches 61.5 ℃ after 30 s of microwave radiation and rapidly rises to 98.5 ℃ at 60 s. This temperature is sufficient to soften asphalt, considering that the softening point of PG 76 is 93 ℃, as mentioned in section 2.1. These results indicate that the functional CG filler exhibits excellent heat generation capability under microwave radiation and has the potential to effectively soften the surrounding asphalt binder. Furthermore, the raw aggregates show minimal temperature fluctuation at different microwave radiation durations (**Fig. 5b**). Their surface temperature only increases by approximately 40 °C after 180 s of microwave heating. This is expected since raw mineral aggregates are generally insensitive to electromagnetic microwave radiation. In contrast, the average temperature of the functional aggregates reaches 90.2 ℃ after just 30 s of microwave radiation, and it rapidly increases to around 107.3 ℃ when the microwave heating time is extended to 60 s. This temperature exceeds the softening point of the asphalt binder, indicating that the functional aggregates can reach temperatures suitable for softening the asphalt binder.

Based on the aforementioned results, it is evident that the CG powder exhibits favorable microwave sensitivity and holds great potential for replacing LM powder to enhance the heating-healing properties of asphalt concrete. Additionally, the functional aggregates demonstrate the ability for rapid heat generation and transfer when incorporated into asphalt concrete. Therefore, the combined usage of CG powder and functional aggregates offers the prospect of high-efficiency heat generation and uniform heat transfer in smart asphalt concrete.

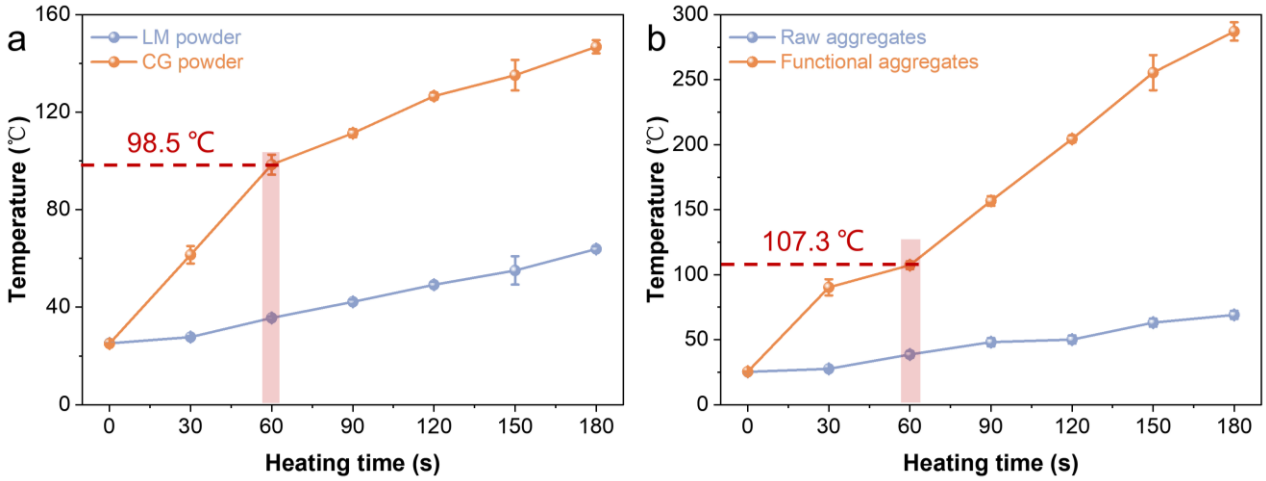

Fig. 5. Microwave heating capacity of raw materials: (a) fillers and (b) aggregates.

3.3.2. Induction heating properties of asphalt concrete under microwave radiation

Infrared images were captured to illustrate the surface temperature distribution of the asphalt concrete samples, as shown in **Fig. 6**. For the PA sample, most regions achieved a relatively low surface temperature of approximately 70 ℃ after 90 s of microwave radiation, which did not reach the optimum healing temperature required to soften the asphalt binder used in this study. In contrast, the PA-50CG sample exhibited a surface covered by green and yellow colors, with the highest surface temperature reaching around 80 ℃ at 90 s. This indicates that the PA-50CG sample possesses superior heating properties compared to the PA sample. By increasing the content of CG powder, the heating effect was further enhanced in the PA-100CG sample, with the highest temperature reaching about 90 ℃ at 90 s, resulting in increased temperature in the surrounding area. Furthermore, in the PA-FAg samples, a large portion of the surface turned red, and the highest surface temperature reached 117 ℃ after 90 s of microwave radiation. Notably, both the PA-FAg-CG50 and PA-FAg-100CG samples achieved surface temperatures of around 110 ℃ after only 60 s of microwave radiation. The blue area became narrower, and the yellow (red) areas expanded, almost covering the entire surface of the samples in the PA-FAg-100CG sample. This indicates that the PA-FAg-CG100 sample exhibits an excellent microwave thermal heating rate and uniformity. However, it is important to note that a temperature exceeding 140 ℃ is likely to result in asphalt deterioration. Therefore, the PA-FAg-100CG sample appeared to collapse at 90 s, emphasizing the need to control the duration of microwave irradiation appropriately.

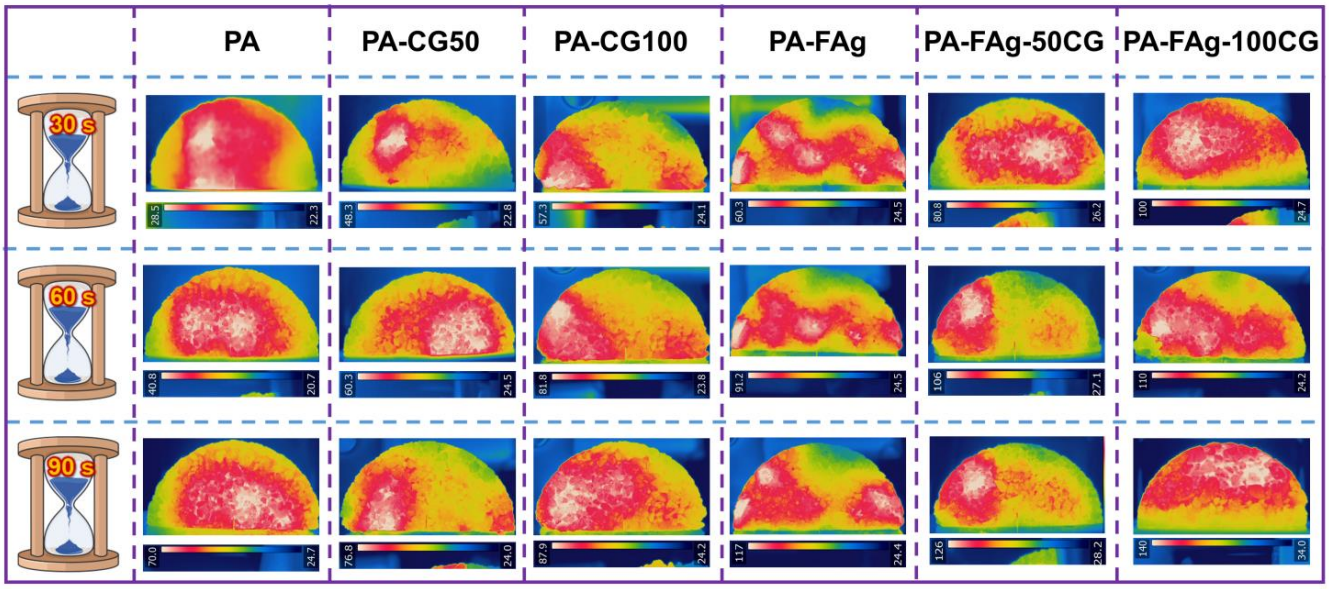

Fig. 6. The surface temperature distribution of the asphalt concrete.

The average surface temperature of the asphalt concrete samples was measured during various durations of microwave radiation to evaluate their microwave heating capacity. As expected, the average temperature of all samples increased with longer microwave heating times. The functional CG-modified asphalt concrete showed an increasing trend in average temperature with higher CG powder content, and the PA-100CG sample achieved the highest average temperature of 114.7 ℃ at 180 s. The PA-100CG and PA-50CG samples exhibited temperature increases of 30-50 ℃ and 20-40 ℃, respectively, compared to the PA samples, indicating that the addition of CG powder improves the microwave heating capacity. This can be attributed to the metal oxide component present in CG powder, which enhances microwave absorption ability (Li, F. et al., 2023; Li et al., 2022). Additionally, the average surface temperature of the PA-FAg, PA-FAg-50CG, and PA-FAg-100CG samples all exceeded 95 ℃ at 60 s. Therefore, a heating time of 60 s was chosen for comparing the microwave heating capacity of different specimens. It is worth noting that some PA-FAg-50CG and PA-FAg-100CG samples appeared loose and collapsed after continuous heating for 90 s, so temperature data was not collected for these samples. Notably, the average surface temperature of the PA-FAg-50CG and PA-FAg-100CG samples increased to 108.6 ℃ and 119.1 ℃, respectively, after 60 s of microwave heating. The calculated surface heating rate for the PA-FAg-50CG and PA-FAg-100CG samples was 1.206 ℃/s and 1.445 ℃/s (**Fig. 7b**), which are the highest reported values to date. It is important to mention that the heating rate and surface temperature of functional aggregate-based asphalt concrete can be easily adjusted by microwave parameters such as power and heating time, depending on the softening point of the asphalt binder.

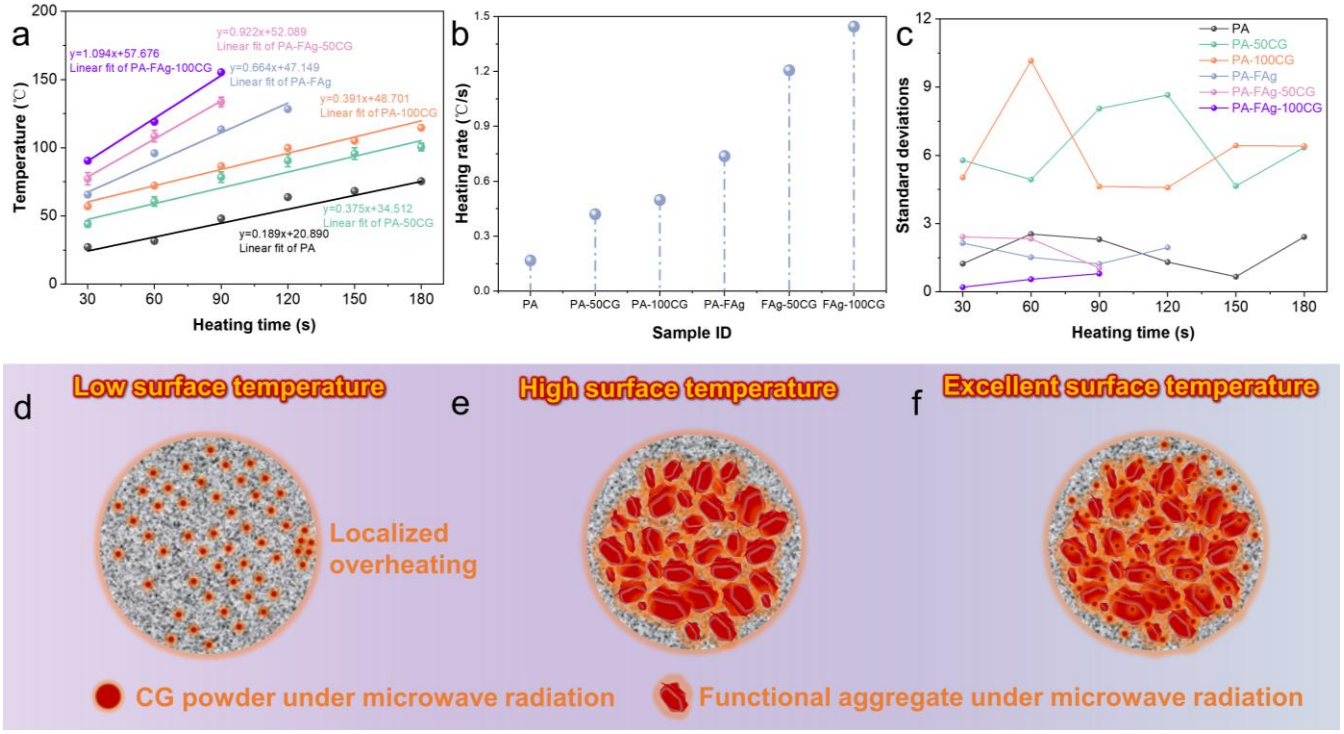

Fig. 7. Surface temperature of asphalt concrete: (a) average temperature; (b) heating rate; (c) SD values; and illustration of heat transfer in the sample containing (d) CG powder; (e) functional aggregates; and (f) CG and functional aggregates.

The standard deviations (SD) of the surface temperature of asphalt concrete were calculated to assess temperature uniformity. The plain asphalt concrete samples showed SD values ranging from 1.0 to 2.5 ℃, indicating relatively uniform heating across these samples (**Fig. 7c**). However, the PA-50CG and PA-100CG samples exhibited higher SD values compared to the plain samples. This suggests that the addition of CG powder to LM powder can cause non-uniform heating, mainly due to the agglomeration of CG powder, leading to localized overheating in regions with a higher concentration of CG powder, while other regions experience slower and restricted heating (**Fig. 7d**). On the other hand, the asphalt concrete samples containing functional aggregates demonstrated low SD values below 3.0 ℃, particularly in the case of PA-FAg-50CG and PA-FAg-100CG samples, where SD values were further reduced to 0.5-2.5 ℃. These results highlight the significance of establishing a three-dimensional functional skeleton structure within the asphalt concrete (**Fig. 7c**). The combined usage of functional aggregates and CG powder facilitates the formation of a distribution system within the asphalt concrete, enabling uniform heating and efficient heat transfer to the surroundings (**Fig. 7f**). This uniform and efficient heating is highly desirable for microwave heating and healing applications. Based on these findings, it can be concluded that the combined usage of functional aggregates and CG filler in asphalt concrete exhibits excellent heating efficiency and uniform heating, making it highly promising for practical applications.

3.4. Evaluation of the heating-healing performance of asphalt concrete

3.4.1. Influence of functional filler on the heating-healing performance

In **Fig. 8a**, the maximum force of the asphalt concrete samples is shown, representing one of the triple repeat tests performed for each sample group. As expected, the maximum force of all samples decreased with an increasing number of damage-healing cycles. **Fig. 8b** presents the HI values calculated for each sample. For the plain PA samples, the HI value decreased from 18.6% to 5.2% after five damage-healing cycles, and it further reduced to approximately 0 after six cycles, indicating that plain PA samples have no heating-healing ability after six cycles. In contrast, all CG-modified asphalt concrete samples exhibited higher HI values, indicating enhanced heating-healing capability compared to plain PA samples. This suggests that the use of CG powder instead of LM powder improves the heating-healing efficiency of asphalt concrete, as CG powder has excellent microwave absorption capacity. This finding is consistent with the heating effect and surface temperature results discussed in Section 3.3. Previous studies have reported that CG powder has a higher dielectric constant imaginary part and magnetic conductivity imaginary part compared to LM powder, indicating a stronger ability to absorb electromagnetic waves. This absorption leads to the conversion of electromagnetic loss into heat, resulting in rapid heating-healing ability in asphalt concrete containing CG powder (Hong et al., 2020; Li et al., 2022). Furthermore, the PA-CG50 and PA-CG100 samples achieved HI values of 31.2% and 28.3% after five damage-healing cycles, respectively, and both of their HI values reduced to approximately 20%. This suggests that adding CG powder alone is not an optimal choice for improving the heating-healing efficiency of asphalt concrete, mainly due to the limited volume of filler in the asphalt concrete. It should be noted that the increase in HI value for the PA-CG100 samples compared to the PA-CG50 samples at any damage-healing cycle is minimal, primarily attributed to the inferior dispersion of 100% CG powder in the asphalt concrete. In such cases, the continuous damage-healing process can lead to the degradation of the asphalt binder, resulting in low healing efficiency of the asphalt concrete after the sixth cycle.

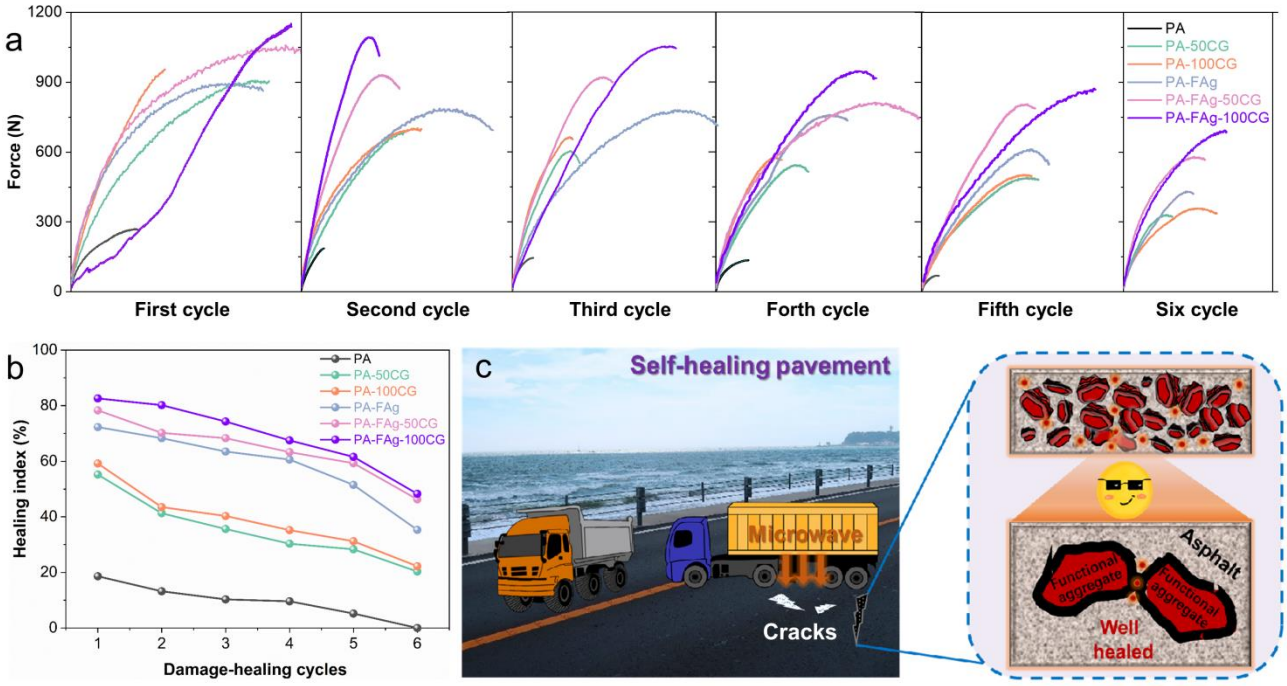

Fig. 8. The heating-healing behaviour of asphalt concrete under microwave radiation: (a) the maximum force; (b) the calculated HI values; and (c) illustration of the heating-healing behaviour of asphalt concrete containing dual functional fillers.

406 *3.4.2. Influence of dual functional additives on the heating-healing performance*

407 In addition, the HI value of the PA-FAg samples reached 72.3% at the first damage-healing cycle,
408 and it reduced to 60.6% after four damage-healing cycles (**Fig. 8b**). Importantly, even after five damage-
409 healing cycles, the HI value of the PA-FAg samples remained above 50%, indicating significant self-
410 healing ability. Encouragingly, the HI value of the PA-FAg samples was still higher than 50% even after
411 five damage-healing cycles, suggesting that the PA-FAg samples showed considerable self-healing ability.
412 Notably, both the PA-FAg-50CG and PA-FAg-100CG samples exhibited remarkably high HI values of
413 78.3% and 82.6%, respectively, at the first damage-healing cycle. Even after five and six damage-healing
414 cycles, their HI values were still around 60% and 50%, respectively. This indicates that the combined
415 usage of functional aggregates and CG powder demonstrated excellent heating-healing capability. In this
416 case, the admixed functional aggregates contribute to the formation of a functional skeleton within the
417 asphalt concrete, facilitating the healing of microcracks at the aggregate-asphalt interfaces.
418 Simultaneously, the introduction of coal gangue mixed with asphalt aids in healing the microcracks in the
419 mastic component (as shown in **Fig. 8c**).

420 The significant improvement in the heating-healing capability of the asphalt concrete containing

functional aggregates and CG compared to the asphalt concrete with CG powder alone is attributed to the microwave sensitivity of the functional aggregates. This sensitivity leads to a uniform and rapid increase in temperature throughout the samples, emphasizing the importance of constructing a functional skeleton within the asphalt concrete. Although the increase in healing efficiency of the asphalt concrete with 100% CG powder is not significant compared to samples containing 50% CG powder, it is recommended to use 100% CG as a replacement for LM powder. This recommendation is based on the efficient and valuable reuse of CG powder, as well as the environmental and economic benefits associated with replacing natural LM powder resources. However, it should be noted that the HI values of all asphalt concrete samples experienced a sharp drop in the sixth damage-healing cycle compared to the fifth cycle. This drop suggests that excessive damage-healing cycles can lead to the deterioration of the asphalt film around the aggregate, compromising the integrity of the asphalt samples. Therefore, it is recommended to limit the number of damage-healing cycles to no more than five to ensure reliable self-healing efficiency.

4. Conclusions

This study introduced a novel concept of a dual responsive microwave heating-healing system in asphalt concrete, achieved through the combined utilization of functional aggregates and coal gangue (CG). The developed asphalt concrete with induction heating-healing capabilities exhibited significant improvements in cracking resistance, excellent performance in generating heat under microwave radiation, and remarkable enhancements in healing effectiveness. The key findings are as follows:

(1) The optimal replacement rate of CG powder in the development of asphalt concrete is determined to be 50% to achieve the highest crack resistance. The mechanical strengths of the asphalt concrete samples containing functional aggregates (PA-FAg samples) exhibited a decrease of approximately 10% compared to the plain PA samples. However, the incorporation of both functional aggregates and CG powder can compensate for the minor loss in strength observed in asphalt concrete with the sole use of functional aggregates. The combined utilization of functional aggregates and CG powder in asphalt concrete can ensure acceptable strength and crack resistance, making it suitable for practical applications.

(2) Both the functional aggregates and CG powder, when added to asphalt concrete, exhibited favorable sensitivity to microwave radiation, resulting in high-efficiency heat generation and uniform heat transfer. This was evident in the PA-FAg-CG50 and PA-FAg-100CG samples, which reached an average surface temperature of approximately 110 ℃ after only 60 seconds of microwave radiation. These samples also

demonstrated exceptional microwave thermal heating rates. Notably, the calculated surface heating rates for the PA-FAg-50CG and PA-FAg-100CG samples were approximately 1.2 ℃/s and 1.4 ℃/s, respectively, making them the highest values reported thus far.

(3) Even after undergoing multiple damage-healing cycles, the HI of the asphalt concrete the combined usage of functional aggregates and CG remained significant, reaching approximately 60% and 50% at the fifth and sixth cycles, respectively, implying excellent heating-healing capability. This combined approach results in an effective healing process that helps maintain the integrity and functionality of the asphalt concrete, even after multiple damage-healing cycles. While the healing efficiency of asphalt concrete with 100% CG powder may not be significantly superior to that of samples containing 50% CG powder, it is still recommended to use 100% CG as a replacement for LM powder in developing self-healing asphalt concrete. This recommendation takes into account the efficient and valuable reuse of CG powder, as well as the environmental and economic benefits associated with replacing LM resources.

Acknowledgement

The authors sincerely acknowledge the funding support from Hong Kong Research Grant Council through the GRF project 15209920, GRF project 15220621, and Engineering Research No.JZ22006O. The authors would also like to thank Mr. Paul Choi for his assistance in sample preparation.

Reference

Alvarez, A.E., Martin, A.E., Estakhri, C., 2011. A review of mix design and evaluation research for permeable friction course mixtures. Construction and Building Materials 25(3), 1159-1166.http://dx.doi.org/10.1016/j.conbuildmat.2010.09.038

Amani, S., Jahangiri, B., Karimi, M.M., 2023. Performance characterization of asphalt mixtures under different aging levels: A fracture-based method. Construction and Building Materials 383.http://dx.doi.org/10.1016/j.conbuildmat.2023.131126

Amani, S., Kavussi, A., Karimi, M.M., 2020. Effects of aging level on induced heating-healing properties of asphalt mixes. Construction and Building Materials 263.http://dx.doi.org/10.1016/j.conbuildmat.2020.120105

Amin, G.M., Esmail, A., 2017. Application of nano silica to improve self-healing of asphalt mixes. Journal of Central South University 24(5), 1019-1026.http://dx.doi.org/10.1007/s11771-017-3504-y

Bai, X., Wang, L., 2023. Study on mesoscopic model of low-temperature cracking of steel slag asphalt mixture based on random aggregate. Construction and Building Materials 364.http://dx.doi.org/10.1016/j.conbuildmat.2022.129974

Beserra Costa, D., de Medeiros Melo Neto, O., Christiane de Figueiredo Lopes Lucena, L., Elísio de Figueiredo Lopes Lucena, A., Maria Sousa Gonçalves Luz, P., 2023. Effects of recycling agents and methods on the fracture and moisture resistance of asphalt mixtures with high RAP contents. Construction and Building Materials 367.http://dx.doi.org/10.1016/j.conbuildmat.2023.130312

Cao, P., Leng, Z., Shi, F., Zhou, C., Tan, Z., Wang, Z., 2020. A novel visco-elastic damage model for asphalt concrete and its

numerical implementation. Construction and Building Materials 264.http://dx.doi.org/10.1016/j.conbuildmat.2020.120261
Cong, P., Chen, Z., Ge, W., 2023. Influence of moisture on the migration of asphalt components and the adhesion between asphalt binder and aggregate. Construction and Building Materials 385.http://dx.doi.org/10.1016/j.conbuildmat.2023.131513
Dai, Q., Wang, Z., Mohd Hasan, M.R., 2013. Investigation of induction healing effects on electrically conductive asphalt mastic and asphalt concrete beams through fracture-healing tests. Construction and Building Materials 49, 729-737.http://dx.doi.org/10.1016/j.conbuildmat.2013.08.089
Erarslan, N., 2023. Investigation of the tensile-shear failure of asphalt concrete base (ACB) construction materials using a non-linear cohesive crack model and critical crack threshold analysis. Construction and Building Materials 364.http://dx.doi.org/10.1016/j.conbuildmat.2022.129901
Fakhri, M., Ahmadi, T., Shahryari, E., Jafari, M., 2023. Evaluation of fracture behavior of stone mastic asphalt (SMA) containing recycled materials under different loading modes at low temperatures. Construction and Building Materials 386.http://dx.doi.org/10.1016/j.conbuildmat.2023.131566
Franesqui, M.A., Yepes, J., García-González, C., 2017. Top-down cracking self-healing of asphalt pavements with steel filler from industrial waste applying microwaves. Construction and Building Materials 149, 612-620.http://dx.doi.org/10.1016/j.conbuildmat.2017.05.161
Fu, C., Liu, K., Liu, P., Oeser, M., 2022. Experimental and numerical investigation of magnetic converge effect of magnetically conductive asphalt mixture. Construction and Building Materials 360.http://dx.doi.org/10.1016/j.conbuildmat.2022.129626
Gallego, J., Gulisano, F., Contreras, V., Páez, A., 2021. The crucial effect of re-compaction energy on the healing response of hot asphalt mortars heated by microwaves. Construction and Building Materials 285.http://dx.doi.org/10.1016/j.conbuildmat.2021.122861
Gan, Y., Zhang, X., Jiang, Z., Lu, D., Xu, N., Han, L., Han, X., 2021. Cementitious Fillers in Cement Asphalt Emulsion Mixtures: Long-Term Performance and Microstructure. Arabian Journal for Science and Engineering 47(4), 4943-4953.http://dx.doi.org/10.1007/s13369-021-06266-3
García, Á., 2012. Self-healing of open cracks in asphalt mastic. Fuel 93, 264-272.http://dx.doi.org/10.1016/j.fuel.2011.09.009
García, A., Bueno, M., Norambuena-Contreras, J., Partl, M.N., 2013. Induction healing of dense asphalt concrete. Construction and Building Materials 49, 1-7.http://dx.doi.org/10.1016/j.conbuildmat.2013.07.105
Guan, B., Liu, J., Zhao, H., Wu, J., Liu, J., Yang, F., 2019. Investigation of the Microwave Absorption of Asphalt Mixtures Containing Magnetite Powder. Coatings 9(12).http://dx.doi.org/10.3390/coatings9120813
Hong, R.-b., Wu, J.-r., Cai, H.-b., 2020. Low-temperature crack resistance of coal gangue powder and polyester fibre asphalt mixture. Construction and Building Materials 238.http://dx.doi.org/10.1016/j.conbuildmat.2019.117678
Huang, G., Zhang, J., Wang, Z., Guo, F., Li, Y., Wang, L., He, Y., Xu, Z., Huang, X., 2023. Evaluation of asphalt-aggregate adhesive property and its correlation with the interaction behavior. Construction and Building Materials 374.http://dx.doi.org/10.1016/j.conbuildmat.2023.130909
Jahanbakhsh, H., Karimi, M.M., Jahangiri, B., Nejad, F.M., 2018. Induction heating and healing of carbon black modified asphalt concrete under microwave radiation. Construction and Building Materials 174, 656-666.http://dx.doi.org/10.1016/j.conbuildmat.2018.04.002
Jiang, J., Leng, Z., Yang, B., Lu, G., Tan, Z., Han, M., Dong, Z., 2022. Penetration mechanism of the emulsion-based rejuvenator in damaged porous asphalt mixture: Microstructure characterization and 3D reconstruction. Materials & Design 221.http://dx.doi.org/10.1016/j.matdes.2022.111014
Jiang, Q., Liu, W., Wu, S., 2023. Analysis on factors affecting moisture stability of steel slag asphalt concrete using grey correlation method. Journal of Cleaner Production 397.http://dx.doi.org/10.1016/j.jclepro.2023.136490
Jiang, X., Gabrielson, J., Huang, B., Bai, Y., Polaczyk, P., Zhang, M., Hu, W., Xiao, R., 2022a. Evaluation of inverted pavement by structural condition indicators from falling weight deflectometer. Construction and Building Materials 319.http://dx.doi.org/10.1016/j.conbuildmat.2021.125991
Jiang, X., Gabrielson, J., Titi, H., Huang, B., Bai, Y., Polaczyk, P., Hu, W., Zhang, M., Xiao, R., 2022b. Field investigation and numerical analysis of an inverted pavement system in Tennessee, USA. Transportation Geotechnics 35.http://dx.doi.org/10.1016/j.trgeo.2022.100759

Jiang, X., Titi, H., Ma, Y., Polaczyk, P., Zhang, M., Gabrielson, J., Bai, Y., Huang, B., 2022c. Evaluating the performance of inverted pavement structure using the accelerated pavement test (APT). Construction and Building Materials 346.http://dx.doi.org/10.1016/j.conbuildmat.2022.128489

Jiang, X., Zhang, M., Xiao, R., Polaczyk, P., Bai, Y., Huang, B., 2021. An investigation of structural responses of inverted pavements by numerical approaches considering nonlinear stress-dependent properties of unbound aggregate layer. Construction and Building Materials 303.http://dx.doi.org/10.1016/j.conbuildmat.2021.124505

Jiang, X., Zhang, Y., Zhang, Y., Ma, J., Xiao, R., Guo, F., Bai, Y., Huang, B., 2023. Influence of size effect on the properties of slag and waste glass-based geopolymer paste. Journal of Cleaner Production 383.http://dx.doi.org/10.1016/j.jclepro.2022.135428

Jiao, W., Sha, A., Liu, Z., Jiang, W., Hu, L., Li, X., 2020. Utilization of steel slags to produce thermal conductive asphalt concretes for snow melting pavements. Journal of Cleaner Production 261.http://dx.doi.org/10.1016/j.jclepro.2020.121197

Karimi, M.M., Amani, S., Jahanbakhsh, H., Jahangiri, B., Alavi, A.H., 2021. Induced heating-healing of conductive asphalt concrete as a sustainable repairing technique: A review. Cleaner Engineering and Technology 4.http://dx.doi.org/10.1016/j.clet.2021.100188

Karimi, M.M., Jahanbakhsh, H., Jahangiri, B., Moghadas Nejad, F., 2018. Induced heating-healing characterization of activated carbon modified asphalt concrete under microwave radiation. Construction and Building Materials 178, 254-271.http://dx.doi.org/10.1016/j.conbuildmat.2018.05.012

Keshavarzi, B., Kim, Y.R., 2016. A viscoelastic-based model for predicting the strength of asphalt concrete in direct tension. Construction and Building Materials 122, 721-727.http://dx.doi.org/10.1016/j.conbuildmat.2016.06.089

Li, B., Li, A., Chen, X., Nan, X., Li, Z., Qiu, K., Ji, H., 2023. Multi-scale investigation on the adhesion properties of warm-mixed recycled SBS modified asphalt. Construction and Building Materials 377.http://dx.doi.org/10.1016/j.conbuildmat.2023.131129

Li, C., Wu, S., Chen, Z., Tao, G., Xiao, Y., 2018. Improved microwave heating and healing properties of bitumen by using nanometer microwave-absorbers. Construction and Building Materials 189, 757-767.http://dx.doi.org/10.1016/j.conbuildmat.2018.09.050

Li, F., Zhao, X., Zhang, X., 2023. Utilizing original and activated coal gangue wastes as alternative mineral fillers in asphalt binder: Perspectives of rheological properties and asphalt-filler interaction ability. Construction and Building Materials 365.http://dx.doi.org/10.1016/j.conbuildmat.2022.130069

Li, J., Cao, Y., Sha, A., Song, R., Li, C., Wang, Z., 2022. Prospective application of coal gangue as filler in fracture-healing behavior of asphalt mixture. Journal of Cleaner Production 373.http://dx.doi.org/10.1016/j.jclepro.2022.133738

Liu, J., Chen, S., Liu, Q., Wang, Y., Yu, B., 2022. Influence of steel slag incorporation on internal skeletal contact characteristics within asphalt mixture. Construction and Building Materials 352.http://dx.doi.org/10.1016/j.conbuildmat.2022.129073

Liu, J., Wang, Z., Li, M., Wang, X., Wang, Z., Zhang, T., 2022. Microwave heating uniformity, road performance and internal void characteristics of steel slag asphalt mixtures. Construction and Building Materials 353.http://dx.doi.org/10.1016/j.conbuildmat.2022.129155

Liu, S., Jin, J., Yu, H., Gao, Y., Du, Y., Sun, X., Qian, G., 2023. Performance enhancement of modified asphalt via coal gangue with microstructure control. Construction and Building Materials 367.http://dx.doi.org/10.1016/j.conbuildmat.2022.130287

Lu, D., Huo, Y., Jiang, Z., Zhong, J., 2023a. Carbon nanotube polymer nanocomposites coated aggregate enabled highly conductive concrete for structural health monitoring. Carbon 206, 340-350.http://dx.doi.org/10.1016/j.carbon.2023.02.043

Lu, D., Jiang, X., Tan, Z., Yin, B., Leng, Z., Zhong, J., 2023b. Enhancing sustainability in pavement Engineering: A-state-of-the-art review of cement asphalt emulsion mixtures. Cleaner Materials 9.http://dx.doi.org/10.1016/j.clema.2023.100204

Lu, D., Leng, Z., Lu, G., Wang, D., Huo, Y., 2023c. A critical review of carbon materials engineered electrically conductive cement concrete and its potential applications. International Journal of Smart and Nano Materials, 1-27.http://dx.doi.org/10.1080/19475411.2023.2199703

Lu, D., Ma, L.P., Zhong, J., Tong, J., Liu, Z., Ren, W., Cheng, H.M., 2023. Growing Nanocrystalline Graphene on Aggregates for Conductive and Strong Smart Cement Composites. ACS Nano 17(4), 3587-

3597.http://dx.doi.org/10.1021/acsnano.2c10141
Lu, D., Sheng, Z., Yan, B., Jiang, Z., Wang, D., Zhong, J., 2023d. Rheological Behavior of Fresh Cement Composites with Graphene Oxide–Coated Silica Fume. Journal of Materials in Civil Engineering 35(10).http://dx.doi.org/10.1061/jmcee7.Mteng-15428
Lu, D., Shi, X., Wong, H.S., Jiang, Z., Zhong, J., 2022a. Graphene coated sand for smart cement composites. Construction and Building Materials 346.http://dx.doi.org/10.1016/j.conbuildmat.2022.128313
Lu, D., Shi, X., Zhong, J., 2022b. Interfacial bonding between graphene oxide coated carbon nanotube fiber and cement paste matrix. Cement and Concrete Composites 134.http://dx.doi.org/10.1016/j.cemconcomp.2022.104802
Lu, D., Shi, X., Zhong, J., 2022c. Interfacial nano-engineering by graphene oxide to enable better utilization of silica fume in cementitious composite. Journal of Cleaner Production 354.http://dx.doi.org/10.1016/j.jclepro.2022.131381
Lu, D., Shi, X., Zhong, J., 2022d. Nano-engineering the interfacial transition zone in cement composites with graphene oxide. Construction and Building Materials 356.http://dx.doi.org/10.1016/j.conbuildmat.2022.129284
Lu, D., Shi, X., Zhong, J., 2022e. Understanding the role of unzipped carbon nanotubes in cement pastes. Cement and Concrete Composites 126.http://dx.doi.org/10.1016/j.cemconcomp.2021.104366
Lu, D., Wang, D., Wang, Y., Zhong, J., 2023e. Nano-engineering the interfacial transition zone between recycled concrete aggregates and fresh paste with graphene oxide. Construction and Building Materials 384.http://dx.doi.org/10.1016/j.conbuildmat.2023.131244
Lu, D., Wang, D., Zhong, J., 2022f. Highly conductive and sensitive piezoresistive cement mortar with graphene coated aggregates and carbon fiber. Cement and Concrete Composites 134.http://dx.doi.org/10.1016/j.cemconcomp.2022.104731
Lu, D., Wang, Y., Leng, Z., Zhong, J., 2021. Influence of ternary blended cementitious fillers in a cold mix asphalt mixture. Journal of Cleaner Production 318.http://dx.doi.org/10.1016/j.jclepro.2021.128421
Marín-Uribe, C.R., Restrepo-Tamayo, L.M., 2022. Experimental study of the tensile strength of hot asphalt mixtures measured with indirect tensile and semi-circular bending tests. Construction and Building Materials 339.http://dx.doi.org/10.1016/j.conbuildmat.2022.127651
Meng, Y., Zhao, X., Liao, Y., Wei, X., Huang, K., Wang, Z., Lei, J., Deng, S., 2023. Study on long -term influence of oil corrosion on asphalt adhesion properties and the mechanism. Construction and Building Materials 384.http://dx.doi.org/10.1016/j.conbuildmat.2023.131449
Moghadam, M.J., Ajalloeian, R., Hajiannia, A., 2019. Preparation and application of alkali-activated materials based on waste glass and coal gangue: A review. Construction and Building Materials 221, 84-98.http://dx.doi.org/10.1016/j.conbuildmat.2019.06.071
Mojabi, S.A., Abdi kordani, A., Mirbaha, B., 2020. Laboratory investigation of stone matrix asphalt modified with SBS polymer and C25 fiber in using the semi-circular bend geometry (SCB) and moisture susceptibility. Construction and Building Materials 261.http://dx.doi.org/10.1016/j.conbuildmat.2020.120511
Mulugeta Alamnie, M., Taddesse, E., Hoff, I., 2022. Thermo-piezo-rheological characterization of asphalt concrete. Construction and Building Materials 329.http://dx.doi.org/10.1016/j.conbuildmat.2022.127106
Phan, T.M., Park, D.-W., Le, T.H.M., 2018. Crack healing performance of hot mix asphalt containing steel slag by microwaves heating. Construction and Building Materials 180, 503-511.http://dx.doi.org/10.1016/j.conbuildmat.2018.05.278
Salehi Ashani, S., Varamini, S., Elwardany, M.D., Tighe, S., 2022. Investigation of low-temperature cracking resistance of asphalt mixtures by conducting Disc-Shaped Compact Tension (DC(T)) and Semi-Circular Bend (SCB) tests. Construction and Building Materials 359.http://dx.doi.org/10.1016/j.conbuildmat.2022.129275
Song, W., Deng, Z., Wu, H., Xu, Z., 2023. Cohesive zone modeling of I–II mixed mode fracture behaviors of hot mix asphalt based on the semi-circular bending test. Theoretical and Applied Fracture Mechanics 124.http://dx.doi.org/10.1016/j.tafmec.2023.103781
Song, W., Deng, Z., Wu, H., Zhan, Y., 2022a. Extended finite element modeling of hot mix asphalt based on the semi-circular bending test. Construction and Building Materials 340.http://dx.doi.org/10.1016/j.conbuildmat.2022.127462
Song, W., Xu, Z., Xu, F., Wu, H., Yin, J., 2021. Fracture investigation of asphalt mixtures containing reclaimed asphalt pavement using an equivalent energy approach. Engineering Fracture Mechanics

253.http://dx.doi.org/10.1016/j.engfracmech.2021.107892
Song, W., Zou, X., Wu, H., Zhan, Y., 2022b. Effect of RAP and glass fiber on mode I fracture behaviors of ultra-thin friction course. Engineering Fracture Mechanics 275.http://dx.doi.org/10.1016/j.engfracmech.2022.108868
Taheri-Shakib, J., Al-Mayah, A., 2023. A review of microstructure characterization of asphalt mixtures using computed tomography imaging: Prospects for properties and phase determination. Construction and Building Materials 385.http://dx.doi.org/10.1016/j.conbuildmat.2023.131419
Tian, Y., Yan, X., Lu, D., Wang, Z., Zhang, J., Xu, O., Li, W., 2020. Characteristics of the Cement Asphalt Emulsion Mixture With Early-Age Strength and Flowability. Frontiers in Materials 7.http://dx.doi.org/10.3389/fmats.2020.00122
Wang, H., Xiong, R., Zong, Y., Li, L., Guo, H., Wang, Z., Guan, B., Chang, M., 2023. Effect of raw material ratio and sintering temperature on properties of coal gangue-feldspar powder artificial aggregate. Construction and Building Materials 384.http://dx.doi.org/10.1016/j.conbuildmat.2023.131400
Wang, J., Qin, Y., Xu, J., Zeng, W., Zhang, Y., Wang, W., Wang, P., 2020. Crack resistance investigation of mixtures with reclaimed SBS modified asphalt pavement using the SCB and DSCT tests. Construction and Building Materials 265.http://dx.doi.org/10.1016/j.conbuildmat.2020.120365
Wang, L., Shen, A., Wang, W., Yang, J., He, Z., Zhijie, T., 2022. Graphene/nickel/carbon fiber composite conductive asphalt: Optimization, electrical properties and heating performance. Case Studies in Construction Materials 17.http://dx.doi.org/10.1016/j.cscm.2022.e01402
Wang, Y., Lu, D., Wang, F., Zhang, D., Zhong, J., Liang, B., Gui, X., Sun, L., 2020. A new strategy to prepare carbon nanotube thin film by the combination of top-down and bottom-up approaches. Carbon 161, 563-569.http://dx.doi.org/10.1016/j.carbon.2020.01.090
Wang, Z., Dai, Q., Porter, D., You, Z., 2016. Investigation of microwave healing performance of electrically conductive carbon fiber modified asphalt mixture beams. Construction and Building Materials 126, 1012-1019.http://dx.doi.org/10.1016/j.conbuildmat.2016.09.039
Xiao, R., Ding, Y., Polaczyk, P., Ma, Y., Jiang, X., Huang, B., 2022. Moisture damage mechanism and material selection of HMA with amine antistripping agent. Materials & Design 220.http://dx.doi.org/10.1016/j.matdes.2022.110797
Yıldız, K., Atakan, M., 2020. Improving microwave healing characteristic of asphalt concrete by using fly ash as a filler. Construction and Building Materials 262.http://dx.doi.org/10.1016/j.conbuildmat.2020.120448
Yoo, D.-Y., Kim, S., Kim, M.-J., Kim, D., Shin, H.-O., 2019. Self-healing capability of asphalt concrete with carbon-based materials. Journal of Materials Research and Technology 8(1), 827-839.http://dx.doi.org/10.1016/j.jmrt.2018.07.001
Zhang, W., Li, Q., Wang, J., Zhao, Z., Jin, D., 2023. Physical and chemical evaluation of adhesion recovery property of aged high-viscosity asphalt based on specialized composite rejuvenators. Journal of Cleaner Production 414.http://dx.doi.org/10.1016/j.jclepro.2023.137758
Zhu, X., Ye, F., Cai, Y., Birgisson, B., Lee, K., 2019. Self-healing properties of ferrite-filled open-graded friction course (OGFC) asphalt mixture after moisture damage. Journal of Cleaner Production 232, 518-530.http://dx.doi.org/10.1016/j.jclepro.2019.05.353